II CONGRESSO NACIONAL DE ENGENHARIA MECÂNICA
II NATIONAL CONGRESS OF MECHANICAL ENGINEERING
12 a 16 de Agosto de 2002 - João Pessoa – PB

SURFACE DEFORMATION EFFECTS ON FLOW PATTERNS INSIDE LIQUID DROPLETS

Edson G. Moreira Filho - *edson@lmt.coppe.ufrj.br*
Department of Mechanical Engineering, EE/COPPE
Universidade Federal do Rio de Janeiro
Caixa Postal: 68503
21945-970 – Rio de Janeiro, RJ, Brazil

Albino J.K. Leiroz♠ - *leiroz@ime.eb.br*
Department of Mechanical and Materials Engineering
Instituto Militar de Engenharia
22290-270 - Rio de Janeiro, RJ, Brazil

Abstract. *A numerical study of droplet surface deformation effects on the interference generated flow patterns within the liquid-phase of an infinite linear array of spherical droplets in the absence of surrounding convective effects is discussed in the present work. The transient evolution of the flow field, obtained using an axisymmetric vorticity-stream function approach, show the development of two toroidal vortices surrounded by a viscous boundary layer close the liquid-gas interface and by a internal wake in the stream axis region. The evolution of the temperature field is also analyzed. An analytical grid generation procedure is used in order to transform the moving-boundary physical domain into a fixed-boundary computational domain and to cluster points in the droplet surface near field, where pronounced gradients are expected. The transformed equations are discretized using the Finite Difference Method and the resulting system of algebraic equations is solved by iterative methods with local error control. Results indicate that velocity and temperature distribution inside individual stream droplets are significantly different from patterns found for isolated droplets in convective streams. Besides, comparison with results where the droplet surface regression is neglected show that the flow and temperature field developments are delayed by the moving boundary effect.*

Keywords: *Droplet Deformation, Droplet Combustion, Droplet Vaporization, Numerical Methods , Moving Boundary.*

1. INTRODUCTION

The atomization of liquid fuel jets, which usually precede the vaporization and combustion in a wide range of important technological applications, invariably leads to sprays with a large droplet volumetric fraction. Within these dense sprays, interaction effects and deviations from the isolated droplet behavior (Spalding, 1953; 1955) become significant and the multi-dimensionality of the phenomena makes pure analytical treatments not applicable.

Reviews of numerical studies of multi-droplet combustion have been presented covering a broad selection of physical situations and stressing the importance of droplet interaction

---

♠ Author to whom correspondence should be addressed.

(Sirignano, 1993, Annamalai, 1992). Numerical studies share the compromise of addressing the different spatial and time scales present in the multi-droplet combustion phenomena and are usually limited to arrays with a small number of droplets.

Liquid circulation studies for isolated droplets in convective streams show the development of a single toroidal vortex surrounded by a viscous boundary layer and an internal wake (Prakash & Sirignano, 1978). Liquid vaporization effects are initially neglected. Results are used to correlate the vortex strength to the shear stress at the liquid-gas interface. Energy diffusion within the recirculation zone is also shown to follow a one-dimensional behavior due to the circulatory flow pattern. For vaporizing liquid droplets, an integral approach is used in the analysis of the viscous, thermal and species boundary layers (Prakash & Sirignano, 1980). Results show the importance of transient effects and that the temperature distribution within the discrete phase is nonuniform during the droplet lifetime.

A detailed numerical analysis of a spherical droplet suspended by a thin filament in a convective stream (Shih & Megaridis,1995). The filament suspended droplet is a typical setup for reactive and nonreactive experimental studies. Results show the influence of filament on the general liquid internal circulation, which includes the development of secondary vortices. Besides, significant effects of the circulation patterns on the droplet vaporization rate were observed.

In the absence of convective effects, droplet mass vaporization reduction in linear reacting arrays due to interference was found and correlated to interdroplet spacing (Leiroz & Rangel, 1995a; 1995b). Furthermore, the nonconvective quasi-steady results indicate the potential flow solution as a valid approximation for the viscous velocity field, based on a negligible tangential velocity observed along the droplet surface. The droplet surface blowing velocity was found the vary along the liquid-gas interface leading to the observed negligible tangential velocity.

Gas-phase transient results during droplet stream combustion have shown the existence of non-vanishing droplet surface tangential velocities that can lead to shear-induced liquid motion within the dispersed phase (Leiroz, 1996). Nevertheless, similarly to the quasi-steady case, the droplet surface normal velocity was found to vary along the liquid-gas interface. Besides, preferential vaporization near the droplet equatorial plane, that can also induce liquid movement inside the droplet, was also observed. Results also show, for the time intervals investigated, a weak dependence of the droplet mass vaporization rate on the interdroplet spacing.

In the present work, the effect of nonuniform droplet surface regression on the transient motion of liquid inside spherical droplets generated by the presence of significant interference effects in droplet streams under stagnant environment conditions is numerically investigated. Constant thermophysical properties are assumed for the purpose of the calculations. The droplet surface normal velocity dependence on the angular position is neglected for the present work. The transient energy and momentum governing equations, written in vorticity-stream function formulation, are discretized using the BTCS Finite Difference scheme (Hoffman, 1992). Results show the temporal evolution of the flow and temperature fields, which are initially compared with patterns found in isolated droplet in convective conditions. Comparisons with results obtained considering uniform droplet surface regression (Moreira Filho & Leiroz, 2000) indicate a delay on the flow and temperature field development for the same conditions.

2. ANALYSIS

In the absence of external convective effects, the study of interactive effects within the dispersed phase of a infinitely long linear array of spherical equidistant droplets, shown in Fig.(1a) can be performed in the solution domain depicted in Fig.(1b). Symmetry considerations around the droplet stream axis, the droplet equatorial plane and the interdroplet mean distance plane are explored in order to simplify of the solution domain.

The flow and energy governing equations are written in nondimensional form, assuming constant thermophysical properties, negligible body forces and secondary convective effects, as

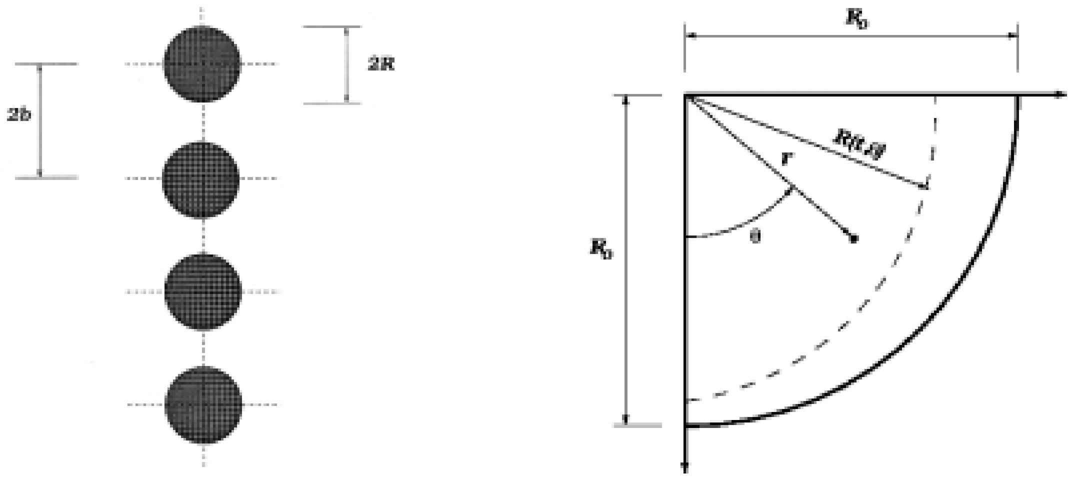

(a) ***(b)***

Figure 1. Sketch of ***(a)*** the center portion of an infinite stream of droplets and ***(b)*** of the physical domain with principal dimensions and deformed droplet surface.

$$\frac{1}{r^2}\frac{\partial}{\partial r}\left(r^2 u_r\right)+\frac{1}{r\,sin\theta}\frac{\partial}{\partial\theta}\left(u_\theta\, sin\theta\right)=0 \tag{1}$$

$$\frac{\partial u_r}{\partial t}+u_r\frac{\partial u_r}{\partial r}+\frac{u_\theta}{r}\frac{\partial u_r}{\partial\theta}-\frac{u_\theta^2}{r}=-\frac{\partial p}{\partial r}+\frac{1}{Re_o}\left[\frac{1}{r^2}\frac{\partial^2}{\partial r^2}\left(r^2 u_r\right)+\frac{1}{r^2\,sin\theta}\frac{\partial}{\partial\theta}\left(sin\theta\frac{\partial u_r}{\partial\theta}\right)\right] \tag{2}$$

$$\frac{\partial u_\theta}{\partial t}+u_r\frac{\partial u_\theta}{\partial r}+\frac{u_\theta}{r}\frac{\partial u_\theta}{\partial\theta}+\frac{u_\theta u_r}{r}=-\frac{1}{r}\frac{\partial p}{\partial\theta}+\frac{1}{Re_o}\left[\frac{1}{r^2}\frac{\partial}{\partial r}\left(r^2\frac{\partial u_\theta}{\partial r}\right)+\frac{1}{r^2}\frac{\partial}{\partial\theta}\left(\frac{1}{sin\theta}\frac{\partial\left(u_\theta\, sin\theta\right)}{\partial\theta}\right)+\frac{2}{r^2}\frac{\partial u_r}{\partial\theta}\right] \tag{3}$$

$$\frac{\partial T}{\partial t}+u_r\frac{\partial T}{\partial r}+\frac{u_\theta}{r}\frac{\partial T}{\partial\theta}=\frac{1}{Pe_o}\left\{\frac{1}{r^2}\frac{\partial}{\partial r}\left(r^2\frac{\partial T}{\partial r}\right)+\frac{1}{r^2\,sin\theta}\frac{\partial}{\partial\theta}\left(sin\theta\frac{\partial T}{\partial\theta}\right)\right\} \tag{4}$$

with boundary conditions

$$u_\theta=u_{\theta,s}(\theta),\; u_r=u_{r,s}(\theta),\; T=1;\; r=R(t,\theta),\; 0<\theta<\pi/2 \tag{5}$$

$$u_\theta=0,\frac{\partial u_r}{\partial\theta}=0,\;\frac{\partial T}{\partial\theta}=0;\;\theta=0,\;\; 0\le r\le R(t,\theta) \tag{6}$$

$$u_\theta = 0\,, \frac{\partial u_r}{\partial \theta} = 0\,, \; \frac{\partial T}{\partial \theta} = 0\,;\; \theta = \pi/2\,, 0 \le r \le R(t,\theta) \tag{7}$$

and initial conditions

$$u_\theta = 0\,,\; u_r = 0\,, T = 0\,;\; 0 \le r \le 1,\; 0 \le \theta \le \pi/2 \tag{8}$$

which corresponds to the instantaneous injection of the droplet stream into an surrounding gas environment.

The nondimensional variables in Eqs. (1-8) are defined as

$$r = \frac{r^*}{R_o}\,;\; u_\theta = \frac{u_\theta^*}{u_{s,max}^*}\,;\; u_r = \frac{u_r^*}{u_{s,max}^*}\,;\; p = \frac{p^*}{\rho(u_{s,max}^*)^2}\,;\; t = \frac{t^*}{R_o / u_{s,max}^*}\,;\; T = \frac{T^* - T_0^*}{T_s^* - T_0^*} \tag{9}$$

where the initial droplet radius (R_o) and the maximum tangential velocity along the droplet surface $(u_{s,max}^*)$ are used as length and velocity characteristic quantities, respectively.

According to the nondimensional variables defined in Eq. (9), the Reynolds (Re_o), Prandtl (Pr) and Peclet (Pe_o) numbers are defined as

$$Re_o = \frac{u_{s,max}^* R_o}{\nu}\,;\; Pr = \frac{\nu}{\alpha}\,;\; Pe_o = Re_o \cdot Pr \tag{10}$$

where ν and α represent the kinematic viscosity and the thermal diffusivity, respectively. In the present work, a droplet surface regression rate is specified and a corresponding droplet surface blowing velocity calculated. A coupled analysis of the liquid and gaseous regions, which allows the appropriate determination of the droplet surface blowing velocity, is currently being studied.

In order to decouple the pressure and velocity fields and reduce the number of equations necessary for the flow analyses, the primitive variable formulation described by Eqs. (1-3) are rewritten in vorticity-stream function form as

$$\frac{\partial \xi_\phi}{\partial t} + u_r \frac{\partial \xi_\phi}{\partial r} + \frac{u_\theta}{r}\frac{\partial \xi_\phi}{\partial \theta} = \frac{\xi_\phi}{r}\left(u_r + u_\theta \cot\theta\right) + \frac{1}{Re_o}\left\{\frac{1}{r^2}\frac{\partial}{\partial r}\left(r^2 \frac{\partial \xi_\phi}{\partial r}\right) + \frac{1}{r^2}\frac{\partial}{\partial \theta}\left[\frac{1}{\sin\theta}\frac{\partial}{\partial \theta}\left(\xi_\phi \sin\theta\right)\right]\right\} \tag{11}$$

$$-\xi_\phi = \frac{1}{r^2 \sin\theta}\frac{\partial}{\partial r}\left[r^2 \frac{\partial}{\partial r}\left(\frac{\psi}{r}\right)\right] - \frac{1}{r^3}\frac{\partial}{\partial \theta}\left[\frac{1}{\sin\theta}\frac{\partial \psi}{\partial \theta}\right] \tag{12}$$

with boundary conditions

$$\frac{\partial \psi}{\partial \theta} = u_{r,s}(\theta)\, r^3 \sin(\theta)\,;\; r = R(t,\theta),\; 0 < \theta < \pi/2 \tag{13}$$

$$\psi = 0\,,\; \xi_\phi = 0\,;\; \theta = 0\,,\; 0 \le r \le R(t,\theta) \tag{14}$$

$$\psi = 0 \, , \; \xi_\phi = 0 \, ; \; \theta = \pi/2 \, , \; 0 \le r \le R(t,\theta) \tag{15}$$

and initial conditions

$$\psi = 0 \, , \; \xi = 0 \, ; \; 0 \le r \le 1 \, , 0 < \theta < \pi/2 \tag{16}$$

Vorticity (ξ_ϕ) and stream function (ψ) are respectively defined by the radial and tangential velocity components as

$$\xi_\phi = \frac{1}{r}\frac{\partial}{\partial r}(ru_\theta) - \frac{1}{r}\frac{\partial u_r}{\partial \theta} \tag{17}$$

and

$$u_r = \frac{1}{r^2 \sin\theta}\frac{\partial \psi}{\partial \theta} \, ; \; u_\theta = -\frac{1}{r\sin\theta}\frac{\partial \psi}{\partial r} \tag{18}$$

The vorticity value at the liquid-gas interface is initially unknown and is determined by an iterative solution procedure applied to Eqs.(10-15), which also accounts for the treatment of the non-linear terms present in Eq.(10).

3. NUMERICAL CONSIDERATIONS

In order to improve solution convergence and control computational costs, clustering of points in the radial direction close to the liquid-gas interface is introduced. The clustering of points is motivated by the high solution gradients expected close to the droplet surface. During the grid generation procedure, an analytical transformation expressed by (Anderson *et al.*, 1984)

$$\eta = 1 + \frac{1}{\tau}\sinh^{-1}\left[(r-1)\sinh(\tau)\right] \tag{19}$$

is applied, where the clustering parameter τ allows the control of the radial point distribution. Analytically obtained metrics are used to rewrite Eqs. (4), (11) and (12), using the introduced transformed variable η.

The numerical treatment of the droplet surface regression is also achieved by the introduction of an analytical transformation of variables expressed by (Rangel & Bian, 1995)

$$\Gamma = R_o t \tag{20}$$

$$w(t,\theta) = \frac{4}{\pi}\tan^{-1}\left(\frac{\eta}{\eta_S(t,\theta)}\right) \tag{21}$$

where $\eta_S(t,\theta)$ corresponds to the instantaneous shape and position of the droplet surface. Due to the singularity present in Eq.(21) for $\eta_S(t,\theta) = 0$, numerical calculations are performed until the droplet size is reduced to a predefined value. Besides, since secundary breakup of the liquid droplets are not being considered in the present model, calculations are limited to time intervals prior to the appearance of an inflexion point along the liquid-gas interface.

The transformed equations are discretized into algebraic form using a BTCS Finite-Difference scheme (Anderson *et al.*, 1984). The resulting system of algebraic equation is solved by iterative methods with local error control. Once convergence is achieved, Eq.(19-21) are analytically inverted and the solution profiles within the physical domain are obtained. Discretizing grids within the physical domain are depicted in Fig.(2) for different times. Regularly spaced grids are recovered for vanishing clustering parameters values. For the present work, the dependence on the angular position of the velocity tangential component along the droplet surface is obtained from gas-phase transient calculations (Leiroz, 1996).

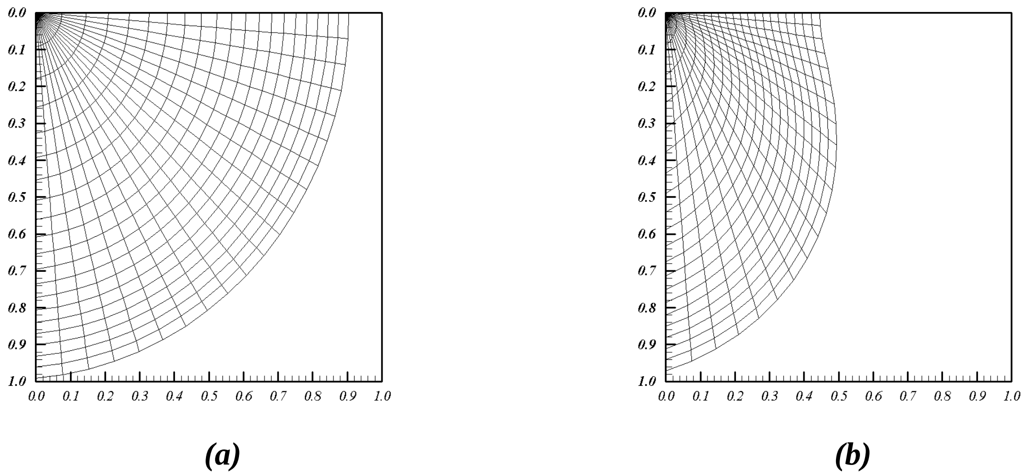

Figure 2: Discretizing grid in the physical domain for $\tau = 2.5$, 21×21 points and $u_{r,max} = 10^{-3}$ –***(a)*** $t = 2$ and ***(b)*** $t = 7$.

4. RESULTS

The proposed numerical procedure was initially validated for the limiting case of an isolated droplet for which the droplet surface tangential velocity induced by interference vanishes. For this limiting case, an analytical solution for the energy equation can be obtained neglecting the equation convective terms. A convergence study is also performed in order to calibrate the mesh clustering parameter τ. For the present work, the functional dependence of the droplet surface tangential velocity is obtained from decoupled gas-phase calculations. In order to evaluate the droplet surface deformation effect, an artificially small droplet blowing velocity is used. For the results shown in the present work $u_{\theta,s} = sin(2\theta)$ and $u_{r,max} = 10^{-5}$. Simulations were conducted on 121×121 grids for a tolerance of 10^{-4}, a clustering parameter τ equal to 2.5 and $\Delta t = 10^{-4}$ which allow a 3-digit precision on the depicted results.

The effect of the Reynolds number on the stream-function transient results are shown in Fig.(3) for $t = 1$, $Pr = 10$ indicating the existence of two toroidal vortices within the liquid phase The toroidal vortices are separated by the droplet equatorial plane. Results show that, for the chosen value of t, the flow development is more pronounced for the lower Reynolds. The delay on the flow development can be understood from the thinner boundary layer structure associated with the higher Reynolds which impairs the momentum transfer normal to the droplet surface. A displacement of the vortex center towards to droplet equatorial plane is also observed for higher Reynolds *(Re_o)*. Besides the existence of a boundary layer close to the liquid-gas interface, a wake between the vortex and the droplet stream axis is also observed. Although these structures are also present in the flow pattern found for isolated droplets in convective stream (Prakash

&Sirignano, 1978), the calculated two-vortex pattern is significantly different from the single vortex found for that configuration. Also, results can be used to quantify the vortices strength. The liquid motion effect on the droplet stream transport mechanisms is currently under study. Moreover, a comparison with results obtained neglecting the droplet surface movement (Moreira Filho, 2000) show, for the surface regression case, a *50%* reduction of stream-function values. Besides, comparison with results for uniform radial regression (Moreira Filho & Leiroz, 2000) indicate that the droplet deformation improves flow development. The combined mechanisms of droplet regression and deformation lead, for the conditions studied, to a delay on the development of the flow field as shown in Fig. (4). It should also be mentioned that steady-state results are obtained for $t = 2$ if the regression of the liquid-gas interface is neglected (Moreira Filho, 2000).

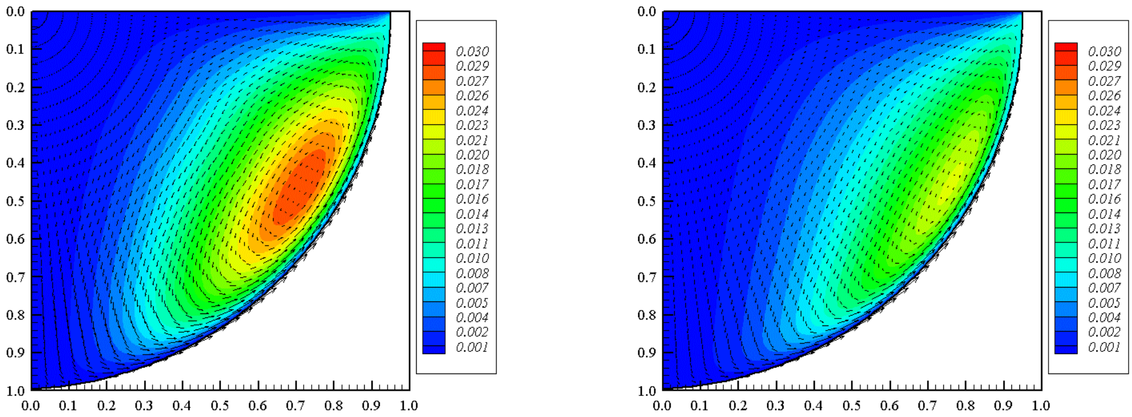

(a) ***(b)***

Figure 3. Stream-function and velocity vectors for $t = 1$, ***(a)*** $Re_o = 10$ and ***(b)*** $Re_o = 100$ — 121×121 grid, $\tau = 2.5$, $u_{\theta,s} = sin(2\theta)$, $u_{r,max} = 10^{-5}$

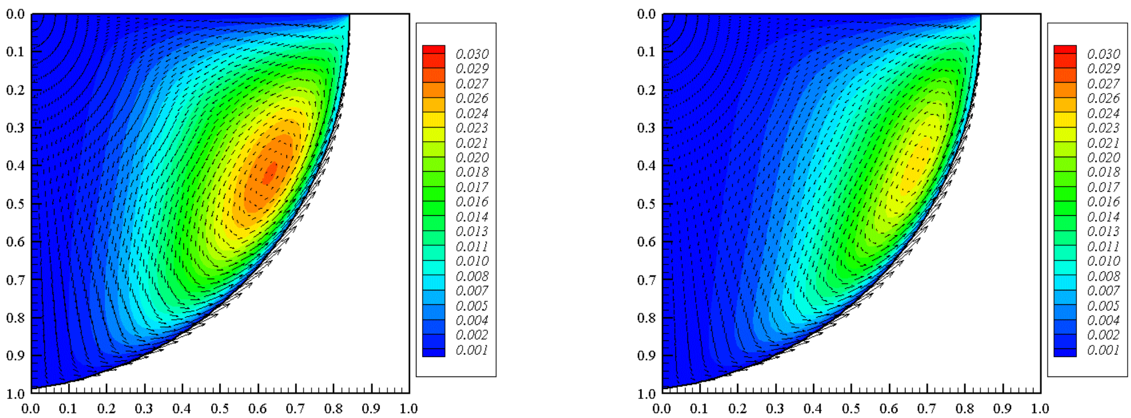

(a) ***(b)***

Figure 4. Stream-function and velocity vectors for $t = 3$, ***(a)*** $Re_o = 10$ and ***(b)*** $Re_o = 100$ — 121×121 grid, $\tau = 2.5$, $u_{\theta,s} = sin(2\theta)$, $u_r = 10^{-5}$

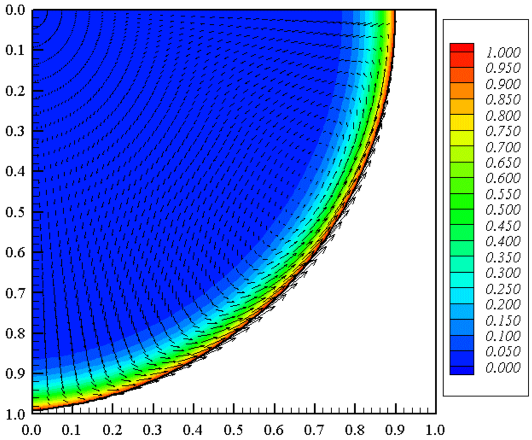

(a)

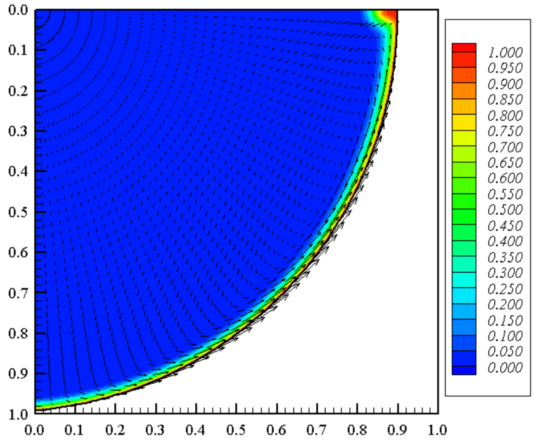

(b)

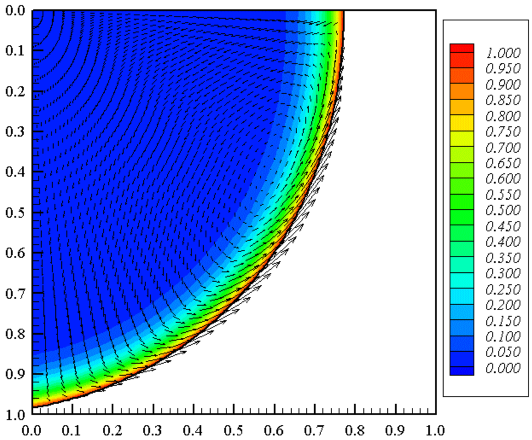

(c)

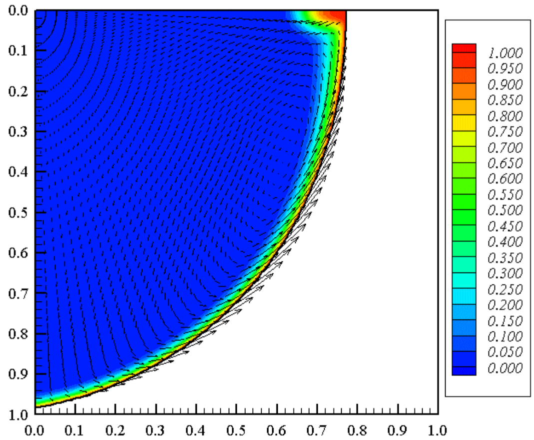

(d)

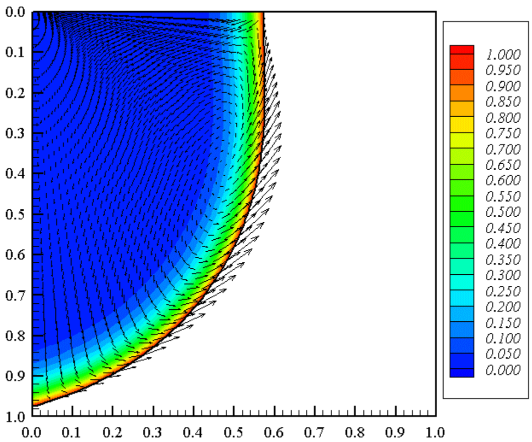

(e)

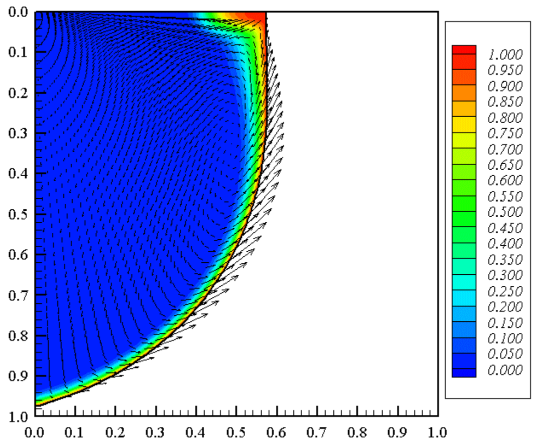

(f)

Figure 4. Temperature field and velocity vectors for $Re_o = 10 - t = 2$ ***(a)***, $t = 4$ ***(c)***, $t = 6$ ***(e)*** – and $Re_o = 100 - t = 2$ ***(b)***, $t = 4$ ***(d)***, $t = 6$ ***(f)*** – -121×121 Grid Points, $u_{\theta,s} = sin(2\theta), u_r = 10^{-5}$.

The evolution of the temperature field is depicted in Fig.(5) for Re_o = *10* and Re_o = *100*. A Prandtl value *(Pr)* of *10*, which is a typical value for liquid fuels, is considered. For initial times, the development of the temperature field presents a weak dependence on the angular position within the liquid droplet as shown in Fig.(5a) for $t = 2$. Despite the almost diffusive behavior associated with early stages of the flow development, a broadening of the thermal boundary layer close to the droplet equatorial plane is observed in Fig. (5b) for Re_o = *100*. For Re_o = *10* a similar quasi-radial behavior of the temperature field is observed as shown in Figs. (5c) and (5e) for $t = 4$ and *6*, respectively. Results obtained considering uniform droplet surface regression indicate for $Re_o = 10$ and for Re_o = *100* a more pronounced temperature field development. The lagging on the temperature field development when droplet deformation is considered is caused by the weakening of the convective effects due to the more intense mass vaporization rate near the droplet equatorial plane. The convective effects on this region associated with the inward motin of fluid is weakened leading to more deficient energy transport. For Re_o = *100* the development of the temperature field is more influenced by inward flow convective effects and a departure from the quasi-radial behavior becomes significant as shown in Figs. (5d) and (5f). The inward motion of fluid observed as θ approach $\pi / 2$ is responsible for the preferential temperature field development. It is worthy mentioning that the nonuniform droplet regression restricts the broadening of the boundary layer to a region closer to the droplet equatorial plane when compared to uniform regression results. Qualitatively, the temperature fields for Re_0 = *10* and Re_o = *100* retain these general behavior for the remaining of the droplet lifetime ($t = 7.2$).

5. CONCLUSIONS

The numerical analysis of the transient convective effects inside liquid droplets in a linear infinite array was performed considering effects of droplet surface regression. Results, which show the importance of transient effects, are used to draw qualitative results of the flow and temperature development characteristics. The existence and development of two toroidal vortices, which contrasts with the single vortex structure found for isolated droplet in convective streams, is show to have a strong effect on the temperature field development. Besides, the influence of the droplet vaporization and the consequential liquid-gas interface regression is shown to have a lagging effect on the flow and temperature field developments. Further studies are necessary to quantify the droplet interaction with linear arrays of droplets considering gas and liquid transient behavior simultaneously.

6. ACKNOWLEDGMENT

The authors would like to acknowledge the financial support provided by the CNPq (Grant No. 520315/98-7). Computer resources were allocated by the Aerodynamics and Thermosciences Laboratory of the *Instituto Militar de Engenharia*.

7. REFERENCES

Anderson, D. A., Tannehill, J. C. and Pletcher, Richard H., 1984; “Computational Fluid Mechanics and Heat Transfer”, Hemisphere Publishing Corporation.

Annamalai, K, 1992.; “Interactive Process in Gasification and Combustion. Part I: Liquid Drop Arrays and Clouds”, Progress Energy Combust. Science, Vol.18, pp.221-295.

Hoffman, J. D. , 1992; “Numerical Methods for Engineers and Scientists”, McGraw-Hill.

Leiroz, A.J.K. and Rangel, R.H., 1995; "Numerical Study of Droplet-Stream Vaporization at Zero-Reynolds Number", Numerical Heat Transfer, Applications, Vol.27, pp.273-296.

Leiroz, A.J.K. and Rangel, R.H. , 1995; "Interference Effects on Droplet Stream Comb.", Proc. 8th Int. Symp. on Transport. Phenomena in Combustion, San Francisco.

Leiroz, A.J.K. , 1996; "Numerical Study of Droplet-Stream Vaporization and Combustion", Ph.D. Dissertation, University of California, Irvine.

Moreira Filho, E.G. and Leiroz, A.J.K., 2000; "Numerical Study of Liquid Internal Circulation During Droplet-Stream Combustion", Brazilian Conference on Mechanical Engineering – CONEM 2000, Natal, RN, Brazil.

Moreira Filho, E.G., 2000; "Analysis of Convective Effects Inside Liquid Droplets in Dense Linear Arrays", M.Sc. Dissertation, Instituto Militar de Engenharia, Rio de Janeiro, Brazil. (in Portuguese)

Moreira Filho, E.G. and Leiroz, A.J.K., 2000, "Numerical Investigation of Surface Regression Effects on Interference Generated Flow Patterns Inside Liquid Droplets", 8^{th} Brazilian Congress of Thermal Engineering and Sciences - ENCIT 2000, Porto Alegre, RS, Brazil.

Prakash S. and Sirignano W.A., 1978; "Liquid Fuel Droplet Heating with Internal Circulation", Int. Journal of Heat and Mass Transfer, Vol.21, 885-895.

Prakash S. and Sirignano W.A, 1980; "Theory of Convective Droplet Vaporization with Unsteady Heat Transfer in the Circulating Liquid Phase", Int. Journal of Heat and Mass Transfer, Vol.23, 253-268.

Rangel R.H. and Bian, X.,1995; "Numerical Solution of Inviscid Stagnation-Flow Solidification Problem", Numerical Heat Transfer, Part A, Vol. 28, pp. 589-603.

Shih A.T. and Megaridis C.M., 1995; "Suspended Droplet Evaporation Modeling in a Laminar Convective Enviroment", Combustion and Flame, Vol. 102, pp. 256-270.

Sirignano, W.A., 1993; "Fluid Dynamics of Sprays", Journal of Fluids Engineering., Vol.115, pp.345-378.

Spalding, D.B., 1953; "The Combustion of Liquid Fuels", Proc. 4th International Symposium of Combustion, Cambridge, MA, pp. 847-864, Williams and Wilkins, Baltimore.

Spalding, D.B. , 1955; "Some Fundamentals of Combustion", Butterworths, London.